Magnetoresistance and magnetization study of thulium

Mark Ellerby* and Keith A. McEwen*
Department of Physics, Birkbeck College, University of London, London WC1E 7HX, England

Jens Jensen
Ørsted Laboratory, Niels Bohr Institute, Universitetsparken 5, 2100 Copenhagen, Denmark
(Received 18 September 1997)

The results of a detailed resistance and magnetization study of thulium are presented. From these results we derive a magnetic phase diagram for thulium. The c-axis component of the resistivity is strongly affected by the superzone energy gaps induced by the modulated ordering of the magnetic moments in thulium in agreement with earlier experiments. According to the theory of Elliott and Wedgwood the superzones introduce an increase of the resistivity proportional to the magnetization just below T_N, whereas experimentally the change is found to be quadratic in the magnetization. Except for this principal discrepancy, the experimental results are well accounted for when combining a variational calculation of the resistivity with the magnetic model derived for thulium from neutron scattering experiments. [S0163-1829(98)05009-7]

I. INTRODUCTION

A detailed neutron-diffraction study of thulium was carried out by Koehler *et al.*,[1] who found that below $T_N = 56$ K the magnetic structure is sinusoidally modulated along the c axis, with a wave vector $\mathbf{Q} \simeq (2/7)\mathbf{c^*}$ and with the moments constrained to the c axis. As the temperature is reduced higher-order odd harmonics appear, and in the zero-temperature limit the modulation of the magnetic moments approaches a nearly perfect square wave which is commensurable with the lattice. Hence at zero temperature the structure is ferrimagnetic with the moments being of maximum magnitude and parallel to the c axis in four hexagonal layers followed by three layers with the moments antiparallel to the c axis. These results were later confirmed by Brun *et al.*,[2] who found that the structure only becomes commensurable below ~ 32 K, and that the magnitude of $\mathbf{Q}$ decreases linearly by about 5% between 32 K and T_N.

The most substantial study of the magnetization of thulium was performed by Richards and Legvold.[3] They determined the broad outline of the magnetic phase diagram and confirmed the ferrimagnetic structure determined by the neutron-diffraction experiments. Thulium exhibits a first-order transition from the ferrimagnetic structure to the c-axis ferromagnet at a critical field applied along the c axis. In the commensurable phase the critical field is found to be nearly constant and about 2.8 T. The saturation moment measured by Richards and Legvold was $7.14\mu_B$ per ion where the extra $0.14\mu_B$ may be associated with the polarization of the conduction electrons. Zochowski and McEwen[4] have recently presented results for the variation of the lattice parameters in thulium obtained using capacitance dilatometry. They summarized their results in a magnetic phase diagram which shows some complexity, and they found evidence of a 0.7% increase in the length of the Tm crystal along the c axis on making the transition from the ferrimagnetic to the ferromagnetic state.

In the low-temperature limit the magnetic excitations are spin waves. In the ferrimagnetic phase the spin waves detected by inelastic neutron scattering are found at energies between 8 and 10 meV.[5–7] Since the magnetic periodicity is seven times that of the lattice along the c axis, the spin waves are split into seven closely spaced energy bands. At low temperatures, a relatively strong coupling between the spin waves and the transverse phonons is observed. Including the corresponding magnetoelastic coupling, the random-phase-approximation (RPA) model[8] developed by McEwen *et al.*[7] explains most of the observations made both in the low-temperature spin-wave regime and at elevated temperatures. Although thulium belongs to the heavy end of the rare-earth series the Ruderman-Kittel-Kasuya-Yosida (RKKY)-exchange interaction, proportional to $(g-1)^2 = 1/36$, is weak compared to the crystal-field anisotropy energies. This implies that crystal-field excitations are important in thulium at elevated temperatures, both below and above T_N.

The spin-wave excitations in the ferromagnetic phase induced by an applied field parallel to the c axis, have been compared with the excitations seen in the zero-field phase at low temperatures.[9,10] The analysis shows that both the crystal-field anisotropy and the exchange coupling is rather strongly modified from one phase to the other, and these changes must be related to the large shift in the c-axis lattice parameter (0.7%) observed at the transition.[4]

The earliest resistance study of a single crystal of thulium was performed by Edwards and Legvold.[11] They found that the resistivity parallel to the c axis showed a sharp upturn at T_N. This increase in the c-axis resistivity below T_N is explained by the reduction of the Fermi-surface area perpendicular to the c axis due to the intersection of new zone boundaries produced by the magnetic periodicity. This superzone effect was proposed by Mackintosh.[12] The theory was subsequently worked out in detail by Elliott and Wedgwood,[13,14] who applied the relaxation time approximation and assumed the conduction electrons to be free-electron-like.

Here we report a systematic study of the resistance and

magnetoresistance in thulium, examining two particular geometries both with the applied field B parallel with the c axis. In the longitudinal geometry the current i is parallel to the c axis and in the transverse case i is parallel to the a axis. In addition magnetization measurements were made in order to verify some of the finer aspects of the magnetic phase diagram and to allow consideration of the effects of demagnetization fields. The theory of Elliott and Wedgwood is generalized by using a variational calculation[15] rather than the relaxation time approximation. Although the account of the superzone effect is essentially unchanged, the comparison between theory and experiments is much improved when the result of the variational calculation is combined with the RPA model for Tm derived from the neutron-scattering experiments.[7,9,10]

II. EXPERIMENTAL DETAILS

The crystals of thulium used in this study were cut from the same ingot as that used in Refs. 4,7,9,10 and grown at the Ames Laboratories. The dimensions of the sample used for the magnetization measurements were $6.5\times1.0\times0.2$ mm (mass 0.01212 g) with the c axis parallel to the longest dimension. The longitudinal resistance sample had a cross-sectional area of 0.20 mm^2 and a length (separation between voltage probes) of 4.5 mm. For the transverse resistance sample the corresponding dimensions were 0.35 mm^2 times 5.5 mm.

The magnetization was studied using the 12 T vibrating sample magnetometer (VSM) at Birkbeck College. The operation of the VSM is described in Ref. 16. The resistance and magnetoresistance measurements were made using the four-probe dc method in conjunction with a Keithley 181 nanovoltmeter and Keithley 220 constant current supply: appropriate current reversals were made to eliminate thermoelectric effects. The cryostat was built by Oxford Instruments consisting of a variable temperature insert mounted in a 7 T vertical-field magnet. The temperature was controlled and measured using a calibrated carbon-glass thermometer in conjunction with a Lakeshore DRC-93C Controller.

To ensure the same conditions for each isothermal magnetoresistance and magnetization measurements the samples were heated above T_N (annealed) and then cooled to the required temperature. Measurements as a function of temperature were made while cooling in a constant field.

III. EXPERIMENTAL RESULTS AND THE PHASE DIAGRAM

In Fig. 1 we present the temperature dependence of the resistivity measured in the longitudinal configuration, with field and current along the c axis. Figure 1(a) shows the effect of an applied field. At zero field there is an upturn in the resistivity at $T_N\sim57.0$ K corresponding to the behavior observed by Edwards and Legvold.[11] In contrast, the application of a field $B=4.0$ T along the c axis, which drives the system ferromagnetic, quenches the upturn and the residual zero-temperature resistivity $\rho(T\rightarrow0)$ becomes significantly lower. Figure 1(b) presents a detail of the first derivative of the resistivity with respect to temperature in an applied field of 1.0 T. The figure shows the presence of two anomalies in

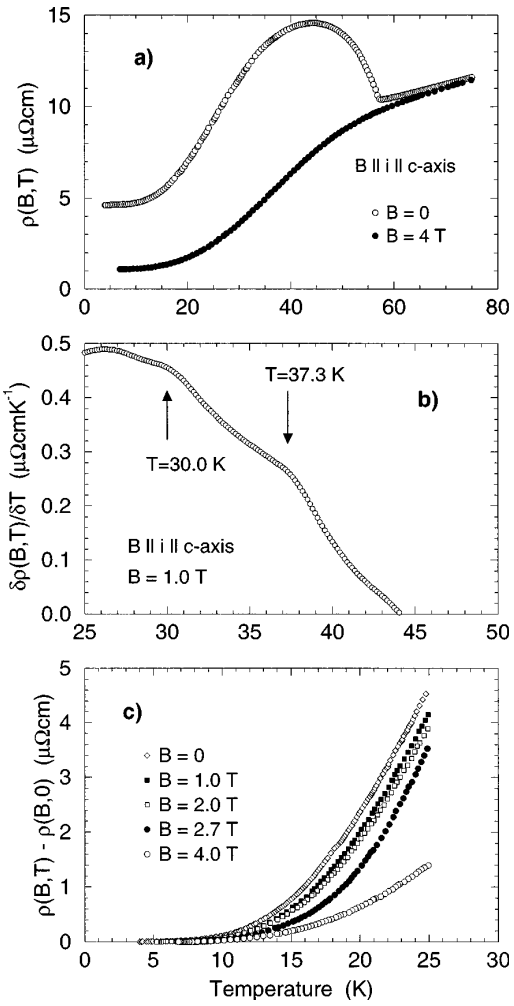

FIG. 1. The temperature dependence of the c-axis resistivity in thulium (a) showing the effect of an applied field; (b) the first derivative for $B=1.0$ T; (c) in various magnetic fields.

the ordered phase at 37.3 and 30.0 K. Evidence of similar transitions was also found in measurements made at other fields between 0 and 2.7 T.[17] The effect of the applied field on the low-temperature behavior of the resistivity is presented in Fig. 1(c): $\rho(T\rightarrow0)$ has been subtracted to ease comparison of data. Between 0 and 2.7 T there is a steady change in the curvature followed by a much more radical change between 2.7 and 4 T, in which interval the system makes the transition from the ferrimagnetic to the ferromagnetic phase.

Figure 2 presents isothermal magnetoresistance and magnetization results obtained at 5 K [Figs. 2(a)–2(c)] and at 35 K [Figs. 2(d)–2(f)]. The samples used for the magnetization and the longitudinal magnetoresistance measurements had a demagnetization factor $D\ll1$ and the consequent demagnetizing fields were negligible. In the transverse configuration [Figs. 2(c) and 2(f)] demagnetization corrections have been made using[18] $D=0.28$. The magnetization data at 5 K show very clearly the transition from the ferrimagnetic phase, with a moment of approximately $1\mu_B$ per ion, to the ferromagnetic phase where the magnetization saturates at a value of $7.14\mu_B$ (in a field of 7 T). The transition occurs at 2.8 T for an increasing field and at about 2.0 T in a decreasing field. At the transition the c-axis resistivity at 5 K [Fig. 2(b)] de-

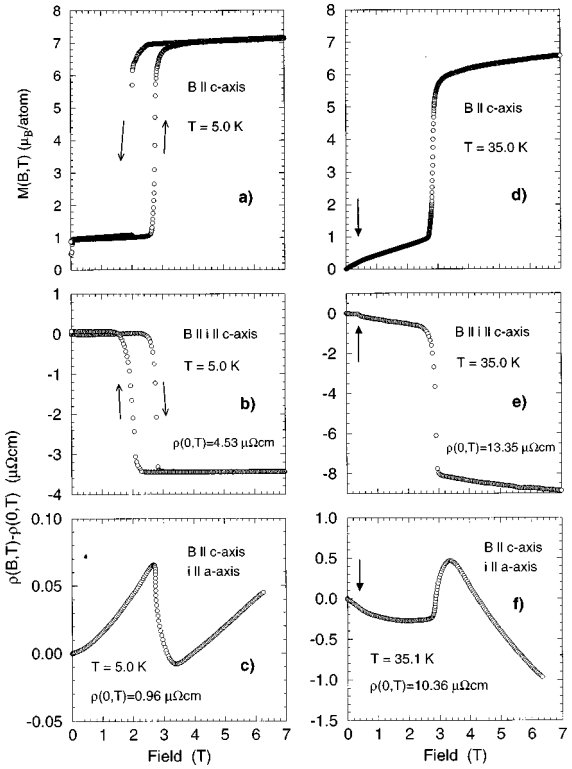

FIG. 2. Isothermal magnetization and longitudinal and transverse magnetoresistance at 5 and 35 K.

creases from approximately 4.6 to 1.1 $\mu\Omega$ cm, whereas the change of the a-axis resistivity [Fig. 2(c)] is one to two orders of magnitude smaller. At low temperatures the transition appears to occur in a single stage for both the magnetoresistance and the magnetization. Figures 2(d)–2(f) show the measurements made at 35 K for an increasing field. The results indicate a low-field transition as marked by arrows at $B=0.4$ T. As the field is increased there is a second transition at 2.8 T after which the magnetization slowly begins to saturate, reaching $6.6\mu_B$/ion at a field of 7 T. The hysteresis in this transition to the ferromagnetic phase was about 0.8 T at 5 K, and decreased to about 0.1 T at 35 K. Note that the transverse magnetoresistance in Fig. 2(f) shows more or less the opposite behavior of that observed at 5 K though on a different scale.

Figure 3 presents the detail and temperature dependence of the low-field transition observed in the temperature interval 33–40 K. The magnetization measurements at 35.0 and 37.0 K clearly shows that there is hysteresis of about 0.3 T associated with this transition, thus indicating that it is of first order. The transition corresponds to the anomaly at 37.3 K in the derivative of the resistivity at 1 T [see Fig. 1(b)].

The relative variations of the resistivities obtained in the present experiments at zero field compare well with the previous results obtained by Edwards and Legvold,[11] but the absolute magnitudes are smaller, by nearly a factor of 2 in the c-axis case and about a factor of 1.3 for the a-axis component. Although we cannot be sure of the origin of these differences, we suspect that they arise from possible errors or variations in the cross-sectional area of the samples in the experiment of Edwards and Legvold. We note that our present results are consistent with the averaged result[19] obtained on a polycrystalline sample.

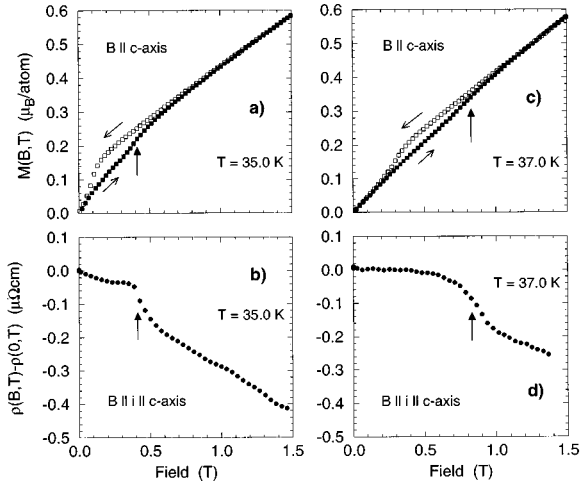

FIG. 3. Details of the low-field transition indicated by an arrow in Figs. 2(d)– 2(f).

Figure 4 presents the magnetic phase diagram derived from the resistivity and magnetization measurements described above. The positions of the phase boundaries were defined by taking the midpoint of a transition for increasing field. The general form of the phase diagram is consistent with that derived from the magnetostriction and thermal-expansion measurements.[4] There are however differences in the details. The first of these differences is the boundary between the ferrimagnetic and ferromagnetic phase. In Ref. 4 there are two additional phases between the two structures within an interval of the field which corresponds to the demagnetization field of 0.8 T not corrected for in that study. The present experiments show that the extra phases do not occur for samples where the demagnetization factor $D \ll 1$, and the transition between the ferrimagnetic and the ferromagnetic phase is accomplished in a single step. Another difference in the two phase diagrams relates to the region marked A in Fig. 4. In the study by Zochowski and McEwen[4] there was an additional phase between A and the c-axis modulated (CAM) phase. The hysteresis and the stepwise change shown by the magnetization, Figs. 3(a) and 3(c), suggests that the demagnetization field, which was significant in the magnetostriction measurements, may also be the cause for this subdivision of the A phase.

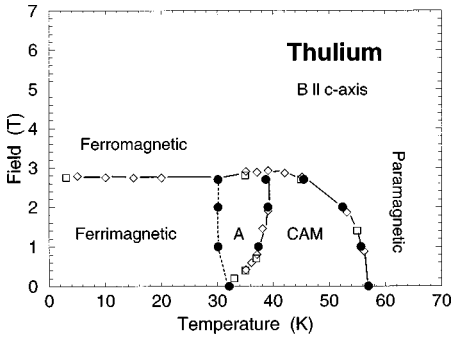

FIG. 4. The magnetic phase diagram constructed from the isothermal magnetization (□), magnetoresistance (◇), and resistance in a constant field (●). The division of the ferrimagnetic phase into two phases at nonzero field, which is indicated by the dashed line, is tentative.

The magnetization measurements at 35 K in Fig. 3(a) [or at 37 K in Fig. 3(c)] indicate that the phase at fields above 0.4 T (or 0.8 T) would have an extrapolated moment of about $0.12\mu_B$/atom (or $0.09\mu_B$/atom) in the limit of zero field. This corresponds very well to the moment expected in the ferrimagnetic phase if it was the stable zero-field phase at these temperatures. Hence, the so-called *A* phase in Fig. 4 must be closely related to the commensurable ferrimagnetic phase found at temperatures below about 30 K, whereas the CAM phase is the incommensurable phase which was observed[2] by Brun *et al.* in the zero-field case. This raises the question concerning the precise nature of the *A* phase, and the significance of the nearly vertical dashed line in Fig. 4 between the ferrimagnetic phase and the *A* phase. One possibility is that the commensurable ferrimagnetic structure has not developed completely in the *A* phase; that this is a mixed phase maintaining some incommensurable features. The other possibility is that the anomalies defining this extra line do not arise from a phase transition but from some other drastic modification of the system. For instance, the superzone gaps induced by the periodic modulated moment may lead to a sudden change in the properties of the conduction electrons, which at zero field may just happen to occur close to the commensurable-incommensurable phase transition. This phase transition is influenced by the applied field, because of the net moment in the commensurable phase, whereas the position and the magnitude of the superzone gaps is only weakly dependent on the field. A neutron-diffraction study of the magnetic structure of thulium in a field parallel to the *c* axis revealed no evidence of any anomalies,[20] in either the wave vector or the intensities of the magnetic satellites (fundamental and third harmonics), at the boundary between the *A* and the ferrimagnetic phases. In contrast, clear anomalies were detected at the boundary between the *A* and CAM phases. Hence, the neutron experiments do not show any indications of the appearance of an extra *A* phase when applying a *c*-axis field.

IV. ANALYSIS OF THE RESISTANCE

Figure 1(a) shows the dramatic effect that magnetic order has on the *c*-axis resistivity. In the zero-temperature limit the residual resistivity is changed by a factor of nearly 4 at the transition from the ferromagnetic phase to the phase with an oscillating *c*-axis moment. The explanation for this behavior is based on the superzone energy gaps created in the conduction electron bands by the oscillating moment, which was considered by Mackintosh.[12] The sinusoidal polarization of the conduction electron spins induced by the RKKY interaction between the spins of the $4f$ electrons and the conduction electrons leads to energy gaps at the wave vectors $(\boldsymbol{\tau}\pm n\mathbf{Q})/2$, where $\boldsymbol{\tau}$ is a reciprocal lattice vector and $\mathbf{Q}$ is the magnetic ordering vector. The leading-order term corresponds to $n=1$, but the squaring up of the magnetic ordering introduces other odd integer values of n, and the higher-order coupling processes introduce both even and odd values of n. In the commensurable case, $\mathbf{Q}=(2/7)\mathbf{c}^*$, the Brillouin zone is reduced by a factor 7 compared to the nonmagnetic one and energy gaps may occur at the center and on the boundaries of the new Brillouin zone. Watson *et al.*[21] have estimated the effects of the magnetic ordering on the band electrons in thulium within a nonrelativistic augmented plane-wave approximation. Their calculations show the appearance of many energy gaps of up to 0.085 eV, at or close to the Fermi energy. These energy gaps result in a large reduction of the Fermi surface area perpendicular to the *c* axis. In order to introduce the essential effects due to the magnetic superzones Elliott and Wedgwood made the simplest possible assumptions in their calculations.[13] They found that the conductivity component (specified by the unit vector $\hat{\boldsymbol{u}}$) perpendicular to the new zone boundary, decreases linearly with the size of the energy gap $\Delta\varepsilon$ in the case where the zone boundary touches the Fermi surface or cuts it into two parts:

$$\sigma_{uu}\simeq\frac{e^2\tau}{4\pi^3}\int_{\varepsilon_{\mathbf{k}}=\varepsilon_F}\frac{(\boldsymbol{v}_{\mathbf{k}}\cdot\hat{\boldsymbol{u}})^2}{|\nabla_{\mathbf{k}}\varepsilon_{\mathbf{k}}|}\,dS\simeq\sigma_{uu}^0(1-\delta_u)\qquad(4.1)$$

assuming a constant relaxation time τ at the Fermi surface, where $\boldsymbol{v}_{\mathbf{k}}$ is the Fermi velocity and dS is a surface element of the Fermi surface. The relative reduction δ_u of the conductivity is to a first approximation the sum of the contributions from all the different energy gaps, among which the dominating terms are those linear in the energy gap. Further, the energy gaps of major importance are those which are proportional to the main first harmonic of the magnetic moments M_1. Hence we may assume

$$\delta_u=\Gamma_u\,M_1/M_1^0,\qquad(4.2)$$

where M_1^0 is the zero-temperature saturation value of the first harmonic. The superzone boundaries are perpendicular to the *c* axis and in the free-electron model the resistivity in the basal plane parallel to the boundaries is only affected to second order in $\Delta\varepsilon/\varepsilon_F$. In principle, the coupling of the electrons to the lattice may introduce linear terms in the basal-plane resistivity, but, experimentally the superzones do not seem to have much effect on the basal-plane resistivity in any of the heavy rare-earth metals.[13,14,22] Edwards and Legvold used the Eqs. (4.1) and (4.2) for analyzing their experimental results on thulium.[11] They used the approximate expressions for the different contributions to τ which were considered by Elliott and Wedgwood.[13] In the fit of the *c*-axis resistivity they used $\Gamma_c=0.86$, and they assumed the basal-plane resistivity to be unaffected by the superzone gaps, $\Gamma_b=0$.

If the effects of the superzones are neglected the Boltzmann equation determining the resistivity may be solved using the variational principle.[15,23,24] Assuming free-electron-like behavior and the RKKY coupling to be $\mathbf{q}$ independent, the magnetic part of the resistivity is[8,24]

$$\rho=\rho_{\mathrm{mag}}^0\int_{-\infty}^{\infty}d(\hbar\omega)\frac{\hbar\omega/k_BT}{4\sinh^2(\hbar\omega/2k_BT)}\sum_\alpha\frac{1}{\pi}\langle\chi''_{\alpha\alpha}(\mathbf{q},\omega)\rangle_{\mathbf{q}}\qquad(4.3)$$

with the weighted $\mathbf{q}$ average of the susceptibility tensor components given by

$$\langle\chi''_{\alpha\alpha}(\mathbf{q},\omega)\rangle_{\mathbf{q}}=\frac{3}{(2k_F)^4}\int_0^{2k_F}qdq\int\frac{d\Omega_{\mathbf{q}}}{4\pi}(\mathbf{q}\cdot\hat{\boldsymbol{u}})^2\chi''_{\alpha\alpha}(\mathbf{q},\omega).\qquad(4.4)$$

In the high-temperature limit these expressions predict the spin-disorder resistivity to saturate at

$$\rho \rightarrow \rho_{\mathrm{spd}} = J(J+1)\rho^0_{\mathrm{mag}}. \tag{4.5}$$

When the scattering of the electrons against impurities and phonons is included the total resistivity is[25]

$$\rho_{\mathrm{total}} = \rho_{\mathrm{res}} + \rho_{\mathrm{phon}} + \rho_{\mathrm{mag}}, \tag{4.6}$$

where the impurity contribution ρ_{res} is considered to be independent of temperature and applied field. The phonon contribution ρ_{phon} is determined by the Bloch-Grüneisen formula[15]

$$\rho_{\mathrm{phon}} = \rho_\Theta \left(\frac{T}{\Theta}\right)^5 \int_0^{\Theta/T} \frac{z^5}{\sinh^2(z/2)}\, dz \tag{4.7}$$

with a Debye temperature[26] of $\Theta = 167$ K in thulium. If the **q** variation of the magnetic contribution (4.4) is neglected it is straightforward to repeat the calculation of Elliott and Wedgwood and include the effect of the superzone boundaries in the variational calculation of the magnetic resistivity contribution. To leading order we may generalize their result and write the final u component of the resistivity as

$$\rho^{uu}_{\mathrm{total}} = \frac{\rho^{uu}_{\mathrm{res}} + \rho^{uu}_{\mathrm{phon}} + \rho^{uu}_{\mathrm{mag}}}{1 - \Gamma_u M_1 / M_1^0} \tag{4.8}$$

with ρ^{uu}_{mag} determined by Eq. (4.3) and $\rho^{uu}_{\mathrm{phon}}$ by Eq. (4.7). The **q** average (4.4) will be affected by the superzones, but the extra effects may be unimportant compared with those already neglected during the derivation of Eq. (4.4). In the case of thulium most of the dispersive effects are weak because of the relatively small magnitude of the RKKY coupling. For instance, the width of the spin-wave energy band at low temperatures amounts to only about 20% of the energy gap in the spin-wave spectrum. Hence, most of the contributions to ρ^{uu}_{mag} are reasonably well described in terms of the mean-field approximation, i.e.,

$$\langle \chi''_{\alpha\alpha}(\mathbf{q},\omega)\rangle_{\mathbf{q}} \simeq \chi''_{\alpha\alpha}(\omega)\big|_{\mathrm{MF}} \tag{4.9}$$

instead of Eq. (4.4). In thulium the mean-field approximation provides a good estimate of the **q** averaging except for two features. Near T_N, the critical fluctuations at small ω for **q** close to **Q** may be so large that they may dominate the behavior of the **q**-averaged susceptibility. Secondly, the dispersive effects cannot be neglected when considering the coupling between the magnetic excitations and the phonons. The coupling between the transverse phonons and the magnetic excitations propagating along the c axis in thulium is important,[7] and there are indications that the same coupling is just as large for the excitations propagating in the basal plane.[9,10] For the purpose of making an order of magnitude estimate of this contribution, $\rho^{uu}_{\mathrm{m\text{-}p}}$, we have assumed the coupling to be isotropic in **q** space and $2k_F$ in Eq. (4.4) to be of the order of $2\pi/c$. These approximations are crude but preserve the essential feature that there is magnetic scattering intensity occurring at all the energies of the phonons, where the low-energy part has an exponentially strong weight in Eq. (4.3) at low temperatures. The mixing of the scattering at different places in **q** space which occurs in the ferrimagnetic phase has two consequences. It makes the calculated results less sensitive to the precise way the weighting in **q** space is performed. Secondly, it increases the volume in the Brillouin zone where low-energy scattering may occur (this being of the order of the factor of 7 by which the Brillouin zone is reduced in the ordered phase). The calculations show that the modification of the magnetic part of the resistivity due to the magnon-phonon interaction is of no importance in the ferromagnetic (or paramagnetic) phase, but that the **q** mixing in the ferrimagnetic phase increases the effect of this coupling so much that its contribution to ρ^{uu}_{mag} is estimated to be the dominating one below ~ 12 K.

The resistivity in the different phases of thulium has been calculated as described above. The mean-field value of the susceptibility tensor used in Eq. (4.9) was obtained in the ferrimagnetic phase from the model established by McEwen *et al.*[7] This model predicts the critical field for the ferri- to ferromagnetic transition to be 4.2 T, which is 50% larger than the experimental value. This discrepancy may be removed by including the large magnetoelastic contribution associated with the 0.7% change of the c-axis lattice parameter which occurs at the transition.[4,9] The neutron-scattering experiments show that the spin-wave energy gap at low temperatures changes from about 8.5 meV in the ferrimagnetic phase to about 6.7 meV in the ferromagnetic phase at a field of 4 T. We have included this shift in the anisotropy energy by introducing, somewhat arbitrarily, the appropriate modification of the crystal-field parameter B_6^0 proportional to $\langle O_6^0 \rangle$. This model is a preliminary one which indicates that the change of the spin-wave energy gap is not necessarily of much importance for the resistivity, since in practice we obtained almost the same result whether the energy shift was included or not.

Figure 5 shows the comparison between the calculated results and the c-axis resistivity measurements in a c-axis field of 0 and 4 T. The resistivity parameters used in the fit are given in Table I, and the calculated contributions to the resistivity in zero field are presented separately in Fig. 6. In this figure the magnetic part is divided into three components, arising from the coupling between the magnetic excitations and the phonons $\rho_{\mathrm{m\text{-}p}}$ the longitudinal part $\rho^{\mathrm{L}}_{\mathrm{mag}}$ due to the cc susceptibility component and the transverse part $\rho^{\mathrm{T}}_{\mathrm{mag}}$ deriving from the sum of the two basal-plane components. Surprisingly, the longitudinal fluctuations dominate, not only close to T_N but also at low temperatures (above 12 K). The variation of the mean field from site to site leads to stronger longitudinal fluctuations in the ferrimagnetic phase at low temperatures than in the ferromagnetic one. Figure 6 indicates that there is still an appreciable variation left in $\rho^{\mathrm{T}}_{\mathrm{mag}}$ and $\rho^{\mathrm{L}}_{\mathrm{mag}}$ at 80 K (notice that in the high-temperature limit $\rho^{\mathrm{T}}_{\mathrm{mag}}$ is going to be twice as large as $\rho^{\mathrm{L}}_{\mathrm{mag}}$). However, considering the total contribution $\rho_{\mathrm{mag}} = \rho^{\mathrm{T}}_{\mathrm{mag}} + \rho^{\mathrm{L}}_{\mathrm{mag}}$ then it is already about 95% of the saturation value ρ_{spd} at T_N and hence the phonon contribution completely dominates the temperature derivative of the resistivity above T_N. In the zero-field case, the resistivity measurements have been extended up to room temperature and the Bloch-Grüneisen formula Eq. (4.7) produces a nearly perfect fit of the data between T_N and room temperature.

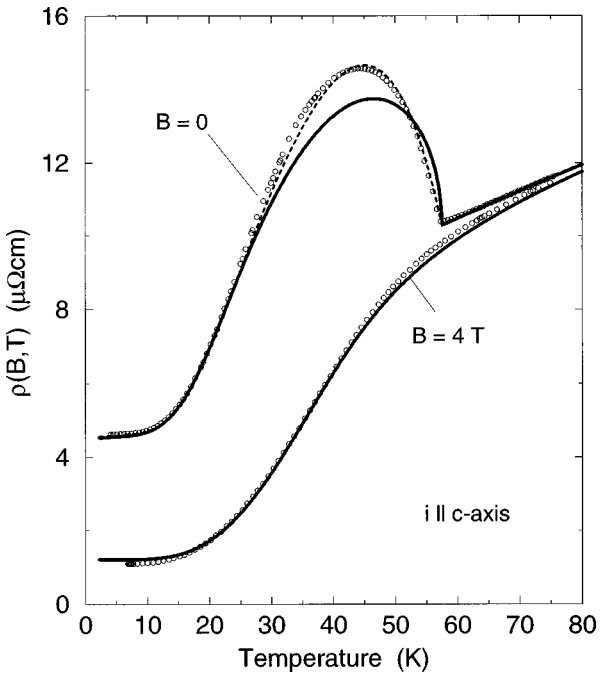

FIG. 5. The c-axis resistivity at zero field and in a field of 4 T applied along the c axis. The experimental results are the same as in Fig. 1(a), which are compared with the calculated behavior shown by the solid lines. The dashed line shows an alternative account of the superzone effects which assumes ρ^{cc}_{total} to be proportional to $(1-\alpha M_1^2)$ instead of using Eq. (4.8).

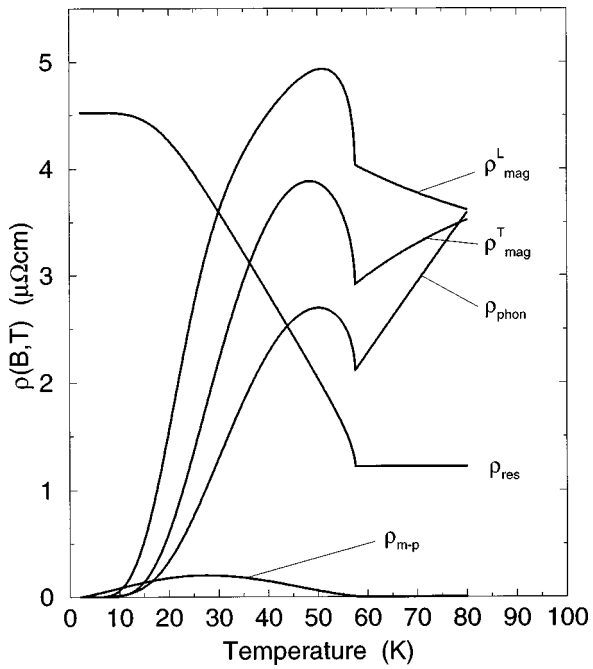

FIG. 6. The different contributions to the calculated variation of ρ^{cc}_{total} at zero field. The impurity term ρ_{res} which is assumed constant when the superzone gaps are neglected, shows the variation of the factor $(1-\Gamma_c M_1/M_1^0)^{-1}$ in Eq. (4.8).

Figure 7 shows the low-temperature behavior of the c-axis resistivity at various fields. The most striking effect here as in Fig. 5 is the strong difference between the c-axis resistivity in the two phases of thulium produced by the superzone energy gaps in the ferrimagnetic phase. There are additional effects due to the reduction of the longitudinal fluctuations and of the contributions due to the magnon-phonon interaction at the transition to the ferromagnetic phase, which lead to a visible change in the low-temperature variation of the resistivity. The good agreement between theory and experiments shown in Fig. 7 indicates that the changes predicted by the theory are indeed occurring.

Figure 8 shows the behavior of the resistivity in the basal plane, and the calculated results at zero field and at 3 T illustrate those differences between the two phases which are still left when the superzone effects are neglected. The comparison with the experimental results at zero field shows a better overall agreement but a less satisfactory account of the low-temperature behavior than obtained in the case of the c-axis resistivity. The low-temperature discrepancy may be due to the fact that the superzone energy gaps in the second order may increase the conductivity in the basal plane. Whether or not this is the right explanation is difficult to say, because the applied field removing the superzone gaps also gives rise to an additional effect not included in the analysis above. Due to the Lorentz force there is an increase of the resistivity in the transverse geometry,[23] which according to Kohler's rule is proportional to the square of the field at low fields. This effect is responsible for most of the field dependence observed at 5 K and shown in Fig. 2(c) and is important in most of the low-temperature regime. The larger changes observed at elevated temperatures and illustrated in Fig. 2(f) are reproduced by the present theory. For instance the slope of the resistivity as a function of field in the ferrimagnetic phase changes sign from being negative between $\sim$15–40 K (opposite sign of the contribution due to the Lorentz force) to being positive above 40 K and below T_N.

TABLE I. Resistivity parameters in units of $\mu\Omega$ cm and Γ_u used in the calculations.

Comp.	ρ_{res}	ρ_Θ	ρ_{spd}	Γ_u
cc	1.22	9.45	7.40	0.73
aa	0.92	31.0	21.2	0

The value of ρ_Θ has been adjusted so that the calculated a-axis resistivity agrees with the experimental one at room temperature. This leads to a less satisfactory fit just above T_N in Fig. 8 than in the c-axis case. One way of removing this discrepancy would be to assume an anisotropic RKKY coupling, so that the contribution ρ^T_{mag} to the a-axis resistivity is enhanced by a factor of about two in comparison with ρ^L_{mag}. However, this seems to be a much too drastic modification of the magnetic properties in comparison with the rather minor change of the a-axis resistivity produced by the modification.

V. DISCUSSION AND CONCLUSION

From the magnetoresistance and magnetization measurements the phase diagram of thulium in the presence of a field in the c direction has been derived. At low temperatures and fields the system is ferrimagnetic, corresponding to a commensurable square-wave modulated ordering of the c component. At high temperatures but below T_N the modulation of the c-axis moment becomes incommensurable with the

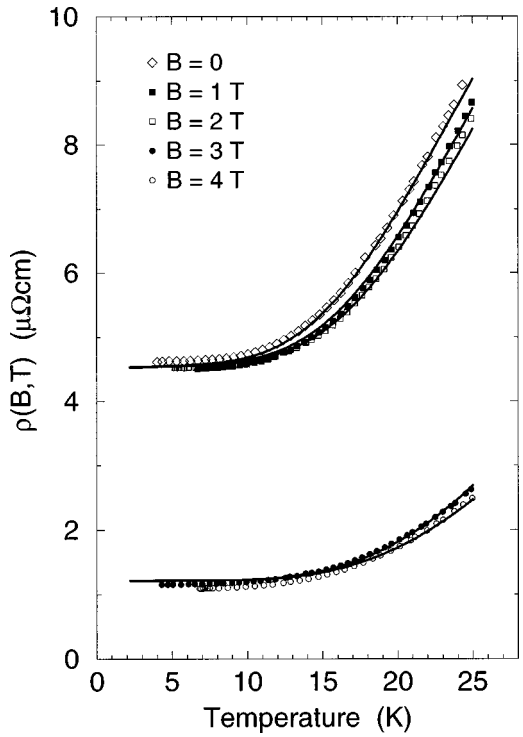

FIG. 7. The comparison between theory and the experimental c-axis resistivity obtained at low temperatures at the different values of the c-axis field. In comparison with Fig. 1(c) the experimental results at 2.7 T (showing a mixed-phase behavior) have been replaced by the results obtained at 3 T, and the residual resistivities have not been subtracted in the present figure.

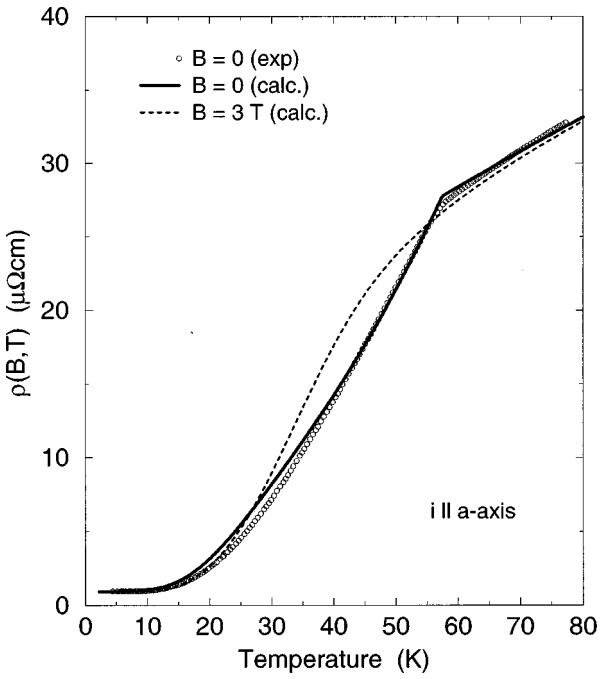

FIG. 8. The experimental and calculated magnetoresistance of thulium when the current is in the a direction.

lattice. The experiments indicate an intermediate A phase between these two phases in the presence of a c-axis field. However, this interpretation is uncertain, and it requires additional experimental investigations to decide whether the anomalies observed in the derivative of the resistivity, or in the thermal expansion,[4] at the boundary between the ferrimagnetic phase and the A phase, are reflecting a true phase transition or are due to other drastic modifications of the system. We note that the neutron-diffraction experiments show no anomalies at this boundary.[20]

The most striking effect observed in the magnetoresistance of thulium is the large change in the c-axis resistivity at the transition between the ferri- and ferromagnetic phases. The superzone gaps reduce the c-axis conductivity by the factor $(1-\Gamma_c)^{-1}=3.7$ in the zero-temperature limit. The description of the magnetoresistance in thulium obtained by the present calculations is satisfactory if the effects of the superzone gaps are small or vanish, as is the case for the a-axis resistivity or for the c-axis resistivity in the ferro- or paramagnetic phase. This circumstance allows an accurate assessment of the superzone effects, which according to the theory of Elliott and Wedgwood[13,14] should scale linearly with the modulated magnetization, Eq. (4.8). The comparison at zero field in Fig. 5 shows that this is roughly true, but there are systematic deviations between the effects predicted by the theory and the observed behavior. The higher odd harmonics developed due to the squaring up of the c-axis moment may give rise to a more complex variation of the superzone energy gaps, but just below T_N the higher harmonics may be neglected, and in this temperature regime the resistivity does not change proportionally to M_1 but rather proportionally to M_1^2 as indicated by the dashed line in Fig. 5. The critical effects expected in this temperature regime seem to be unimportant: at least these effects should enhance the resistivity in comparison with the mean-field behavior rather than the opposite. Thermal activation across the superzone energy gaps neglected in the theory should be unimportant as soon as M_1/M_1^0 is larger than ~ 0.06 (0.1 K below T_N).

Apart from the different influence the superzone energy gaps have on the c-axis resistivity, the present account of the magnetoresistance of thulium is acceptable and it is much improved in comparison with the previous one.[11] The resistance in thulium behaves in a way which is consistent with the RPA model established by McEwen *et al.*[7] The comparison between the theory and the experiments is improved when including the isotropic extrapolation of the magnetoelastic contribution derived for the excitations propagating in the c direction.[7] However, the improvement is marginal because the effect is small and only of slight importance at the very lowest temperatures.

In an anisotropic ferromagnet the longitudinal part of the susceptibility in Eq. (4.3) may be neglected to a first approximation in comparison with the transverse spin-wave contributions. In this case[27,28] the magnetic resistivity becomes proportional to $T\exp(-\Delta/k_BT)$ where Δ is the energy gap in the spin-wave spectrum. At low temperatures thulium is a well-defined spin-wave system, but the approximation which applies for instance in terbium, does not apply here for several reasons. The modulation of the mean field from site to site allows large longitudinal fluctuations in the ferrimagnetic phase and it turns out that the contribution from these fluctuations dominates in the ferrimagnetic phase at temperatures above ~ 12 K. The other reason is the weakness of the exchange coupling compared to the crystalline anisotropy

terms, which implies that poles, other than the spin-wave pole, in the transverse component of the susceptibility tensor rapidly become important when the system is heated.

The present work on thulium has revealed that there is a need for a closer examination of the effects which the modulated magnetic ordering have on the conduction electrons. We have indicated that it should be possible to get a sizable reduction of the Fermi-surface area which is quadratic in the magnetization rather than linear. The recent improvements in the description of the magnetic properties of the other heavy rare-earth metals[8] may be utilized for similar improvements in the analysis of the superzone effects occurring, for example, in the magnetically modulated phases of erbium and holmium.

ACKNOWLEDGMENTS

We thank S. Zochowski, M. de Podesta, and E. Gratz for useful discussions and comments during this study. We acknowledge support from the ESPRC, the Wolfson Foundation, and the Danish Natural Science Research Council.

*Present address: Department of Physics and Astronomy, University College London, Gower Street, London WC1E 6BT, England.

[1] W. C. Koehler, J. W. Cable, E. O. Wollan, and M. K. Wilkinson, Phys. Rev. **126**, 1672 (1962).
[2] T. O. Brun, S. K. Sinha, N. Wakabayashi, G. H. Lander, L. R. Edwards, and F. H. Spedding, Phys. Rev. B **1**, 1251 (1970).
[3] D. B. Richards and S. Legvold, Phys. Rev. **186**, 508 (1969).
[4] S. W. Zochowski and K. A. McEwen, J. Magn. Magn. Mater. **104-107**, 1515 (1992).
[5] J. A. Fernandez-Baca, R. M. Nicklow, and J. J. Rhyne, J. Appl. Phys. **67**, 5283 (1990).
[6] J. A. Fernandez-Baca, R. M. Nicklow, Z. Tun, and J. J. Rhyne, Phys. Rev. B **43**, 3188 (1991).
[7] K. A. McEwen, U. Steigenberger, and J. Jensen, Phys. Rev. B **43**, 3298 (1991).
[8] J. Jensen and A. R. Mackintosh, *Rare Earth Magnetism: Structures and Excitations* (Clarendon, Oxford, 1991).
[9] U. Steigenberger, K. A. McEwen, J. L. Martinez, and J. Jensen, Physica B **180-181**, 158 (1992).
[10] K. A. McEwen, U. Steigenberger, L. Weiss, T. Zeiske, and J. Jensen, J. Magn. Magn. Mater. **140-144**, 767 (1995); (private communication).
[11] L. R. Edwards and S. Legvold, Phys. Rev. **176**, 753 (1968).
[12] A. R. Mackintosh, Phys. Rev. Lett. **9**, 90 (1962).
[13] R. J. Elliott and F. A. Wedgwood, Proc. Phys. Soc. London **81**, 846 (1963).
[14] R. J. Elliott and F. A. Wedgwood, Proc. Phys. Soc. London **84**, 63 (1964).
[15] J. M. Ziman, *Electrons and Phonons* (Clarendon, Oxford, 1962).
[16] M. Ellerby, K. A. McEwen, M. de Podesta, M. Rotter, and E. Gratz, J. Phys.: Condens. Matter **7**, 1897 (1995).
[17] M. Ellerby, Ph.D. thesis, Birkbeck College, London, 1995.
[18] E. C. Stoner, Philos. Mag. **36**, 803 (1945).
[19] R. V. Colvin, S. Legvold, and F. H. Spedding, Phys. Rev. **120**, 741 (1960).
[20] S. W. Zochowski, K. A. McEwen, and P. Burlet (private communication).
[21] R. E. Watson, A. J. Freeman, and J. P. Dimmock, Phys. Rev. **167**, 497 (1968); A. J. Freeman, in *Magnetic Properties of Rare Earth Metals*, edited by R. J. Elliott (Plenum, London, 1972), p. 245.
[22] A. R. Mackintosh and L. E. Spanel, Solid State Commun. **2**, 383 (1964).
[23] M. Kohler, Ann. Phys. (Leipzig) **36**, 906 (1938).
[24] N. Hessel Andersen, J. Jensen, H. Smith, O. Splittorff, and O. Vogt, Phys. Rev. B **21**, 189 (1979).
[25] T. van Peski-Tinbergen and A. J. Decker, Physica (Amsterdam) **29**, 917 (1963).
[26] S. Legvold, in *Magnetic Properties of Rare Earth Metals*, edited by R. J. Elliott (Plenum, London, 1972), p. 335.
[27] A. R. Mackintosh, Phys. Lett. **4**, 140 (1963).
[28] N. Hessel Andersen and H. Smith, Phys. Rev. B **19**, 384 (1979).